ELSEVIER

Chemical Geology 163 (2000) 25–42

CHEMICAL GEOLOGY
INCLUDING
ISOTOPE GEOSCIENCE

www.elsevier.com/locate/chemgeo

# Carbon dioxide mediated dissolution of Ca-feldspar: implications for silicate weathering

Astrid Berg [a,1], Steven A. Banwart [b,*]

[a] *Department of Inorganic Chemistry, The Royal Institute of Technology, 100 44 Stockholm, Sweden*
[b] *Department of Civil and Environmental Engineering, University of Bradford, Bradford BD7 1DP, UK*

Received 17 September 1997; accepted 19 March 1999

**Abstract**

Experimental studies on the dissolution kinetics of anorthite under $N_2$(g) and $CO_2$(g) atmospheres at 25°C in electrolyte solutions, pH range $5.5 < pH < 8.5$, have been performed using laboratory flow-through reactors. Aluminum release from anorthite is accelerated in the neutral to near-basic pH region. Because Al is the slowest dissolving network-forming cation under these conditions, we propose that accelerated Al release corresponds to a long-term acceleration of anorthite dissolution. The rate of Al release from anorthite correlates with solution concentration of carbonate ion according to a fractional-order empirical rate law; $k = (1.1 \pm 1) \times 10^{-7}$ $mol^{0.76}$ $m^{-1.52}$ $h^{-1}$:

$$\text{Rate} = k\left[CO_3^{2-}\right]^{0.24}$$

We propose a two-step reaction mechanism where inorganic carbon is rapidly adsorbed, forming a reactive bi-dentate surface Al–carbonate complex that is released to solution in a much slower, irreversible step. The rate expression formally derived from this dissolution mechanism is consistent with the observed dependence of Al release rate on the master variables $PCO_2$ and pH. A comparison with published data on the weathering kinetics of plagioclase in solutions of oxalic acid shows that the reactivity of carbonate is similar to that of the organic ligand oxalate. Because of pH effects on the speciation of these ligands in solution and on mineral surfaces, carbonate promoted weathering is especially important at near-neutral and basic pH. We propose that the generally termed ''carbonation weathering'', the effect of elevated subsurface $PCO_2$ to accelerate rock weathering through suppression of pH, be extended to include the speciation and reactivity of inorganic carbon at neutral and near-basic pH. 

*Keywords:* Silicate; Weathering; Feldspar; Carbon dioxide; Carbonate; Oxalate

* Corresponding author. Current address: Department of Civil and Structural Engineering, University of Sheffield, Mappin Street, Sheffield S1 3JD, UK.
[1] Current address: Linköpings Universitet, Campus Norrköping, ITUF, Environmental Science, 601 74 Norrköping, Sweden.

0009-2541/00/$ - see front matter 
PII: S0009-2541(99)00132-1

## 1. Introduction

Current models of the geochemical carbon cycle include a weathering feedback mechanism that moderates calculated fluctuations of atmospheric $PCO_2$ (Walker et al., 1981; Berner et al., 1983; Volk, 1987; Marshall et al., 1988; Berner, 1991; Berner, 1994). This negative feedback results from increased weathering of Ca- and Mg-silicates, which provides a long-term sink for atmospheric carbon, in response to increasing atmospheric $PCO_2$. The mechanism is thought to occur through greenhouse and fertilization effects of increased $PCO_2$ on global temperature and vegetation, respectively, and their associated impact to accelerate chemical dissolution in soils.

Chemical models for mineral weathering in soils indirectly address effects of climate and biota by describing how dissolution rates depend on temperature and the composition of soil water. In particular the effects of protons and organic acids, originating from coupled biological production and decomposition, to accelerate dissolution rates (White and Brantley, 1995) are considered (Schnoor and Stumm, 1985).

Elevated carbon dioxide levels have also been observed to increase weathering rates in laboratory studies at high temperature (100–200°C) and $PCO_2$ (2–20 bar) (Lagache, 1965). The weathering rate at these pressures is represented as proportional to $PCO_2^{0.3}$. Models of the geochemical carbon cycle, that mathematically formulate a globally averaged effect of $CO_2$ on weathering, adopt this relation and consequently assume that this same relation holds at $PCO_2$'s encountered in the atmosphere or in natural soils (Walker et al., 1981; Volk, 1987; Marshall et al., 1988; Francois and Walker, 1992). Extrapolation of Lagache's experiments also provide the basis of relations between weathering rate and $PCO_2$ used to model weathering in soils (Warfvinge and Sverdrup, 1992; Sverdrup and Warfvinge, 1993). The effect of $CO_2$ in these experiments has been interpreted as solely a pH effect (Helgeson et al., 1984; Brady, 1991) or as a result of carbon dioxide adsorption (Sverdrup, 1990). Since the mechanism of the effect is not known, and the extrapolation to low $PCO_2$'s values is not verified, additional studies on the implied link between $PCO_2$ and mineral weathering is needed.

It is often postulated that dissolved carbon dioxide provides protons for enhanced mineral dissolution; i.e., ''carbonation weathering'' (Holland et al., 1986; Schlesinger, 1991). The upper range of tabulated soil $PCO_2$ ($10^{-2}$–$10^{-1.5}$ atm) (Appelo and Postma, 1993) only results in suppression of pH to values slightly below pH 5, while acceleration of silicate weathering due to protons generally occurs below pH 4–5. Brady and Carroll (1994) also showed conclusively that at pH 4, weathering of plagioclase at 25°C was not significantly different under $CO_2$ and inert atmosphere. Malmström and Banwart (1997) showed no effect of $CO_2$ on biotite dissolution, while Wogelius and Walther (1991) and Brantley and Chen (1995); citing data from Xie, 1994 showed slower dissolution in the presence of $CO_2$ for olivine and wollastonite, respectively. Bruno et al. (1992), however, observed that iron oxide dissolution is enhanced at neutral pH in the presence of $CO_2$(g). They proposed a ligand-accelerated dissolution mechanism where adsorbed inorganic carbon species de-stabilize the mineral surface. This effect is similar to that proposed for adsorbed organic ligands such as oxalate to accelerated mineral dissolution, and is expected considering the structural similarity between the carbonate ligand and carboxylic acids.

It is clear that adsorbed ligands can influence the stoichiometry and rate of release for framework ions exposed at the surface of dissolving feldspars (see review by Blum and Stillings, 1995). Previous studies of bytownite, labradorite (Welch and Ullman, 1993) and oligoclase (Mast and Drever, 1987) dissolution showed Al release to be slightly slower than for Si for $5 < pH < 9$. Studies with albite showed the dissolution to be more nearly stoichiometric in the same pH range, with slightly faster release of Si (Chou and Wollast, 1984, 1985a; Holdren and Spyer, 1985). All authors generally reported non-stoichiometric dissolution for $pH < 5$, with preferential release of Al observed in all cases. For oligoclase (Mast and Drever, 1987), bytownite and labradorite (Welch and Ullman, 1993), the presence of organic ligands was found to accelerate Al release such that nearly stoichiometric release was obtained in the range $5 < pH < 9$. The dissolution kinetic models of Schnoor (1990) and Malmström and Banwart (1997) predict that accelerating the release rate of the slowest dissolving framework ion will lead to an eventual

accelerated stoichiometric dissolution of the bulk mineral. If Al release is slower than Si release at circumneutral pH, then acceleration of Al release through formation of reactive surface Al-oxalate or Al–carbonate complexes will lead to accelerated dissolution of the mineral.

Here we present laboratory evidence that the weathering rate of calcium feldspar (anorthite; $CaAl_2Si_2O_8(s)$) relates directly to the activity of the carbonate ligand under conditions of pH, temperature and total pressure that approximate those of modern soils. The increase in dissolution rate is significantly greater, at near-neutral pH, than that predicted from the published reactivity of oxalic acid (Amrhein and Suarez, 1988). We conclude that the speciation and reactivity of inorganic carbon should be considered in current models of chemical weathering, and should be assessed regarding a possible role in the weathering feedback mechanism.

## 2. Experimental materials and methodology

### 2.1. Mineral preparation and characterization

Anorthite preparation was carried out at the mineralogy department of the National Natural History Museum (Naturhistoriska Riksmuseet, Stockholm). Centimeter-sized samples of anorthite-rich rock from Grass Valley, CA (Wards Scientific) were picked over to select those with the most uniform visual appearance, excluding samples with darker inclusions or with obvious oxide or carbonate coatings. The selected pieces were crushed, sieved and then passed sequentially through a magnetic separator three times. The white-colored separate was immersed briefly in distilled water to eliminate the greatest part of any fine dust remaining from the grinding procedure, then rinsed three times in succession with sonification in ethanol for 3–5 min each time, and with decanting and replacement of the ethanol used in each rinse. The cleaned powder was then left to air dry. Chemical composition was determined by electron micro probe (Table 1), with results showing no detectable Na. Surface area of the chosen size fraction, 30–70 μm, was determined using the B.E.T. method to be 0.43 $m^2/g$. X-ray powder diffraction analysis of unreacted anorthite samples showed no crystalline phases above the detection-limit of 5% other than anorthite. Scanning electron microscopy (SEM) and SEM backscatter imaging showed no adhering fine material, no surface coatings or films and no visible exsolved phases.

Table 1
Electron microprobe analysis of Grass Valley anorthite

| wt.% | Element | Stoichiometric coefficient |
|---|---|---|
| Al | 18.26 | 1.94 |
| Si | 19.64 | 2.0 |
| Ca | 16.79 | 1.2 |

### 2.2. Flow reactor

The kinetic experiments were performed using a thin-film continuous flow reactor (Bruno et al., 1991; Deng and Banwart, 1994; Malmström and Banwart, 1997). The advantages are similar to fluidized-bed (Chou and Wollast, 1984, 1985a), single-pass mixed-flow (Holdren and Spyer, 1985; Rimstidt and Dove, 1986) and single-pass bed (Knauss and Wolery, 1986) reactors where reaction products are flushed from the reactor to minimize back-reactions with the mineral. The solid phase is introduced as a thin (1–2 mm) layer of powder on a membrane filter across which a feed solution is continuously pumped. Dissolution rate is determined from the product of flowrate and dissolved ion concentration at the reactor effluent, and normalized to B.E.T. surface area of reacting solid mineral. Flowrate is measured by weighing effluent sampled during a controlled interval of time. This reactor is, in concept, a differential cross-section taken perpendicular to the longitudinal axis of an experimental column. The experimental reaction rates represent an average rate of solute accumulation within the reactor during the sampling interval, and are representative if rates are approximately steady over the sampling interval.

### 2.3. Experimental and analytical procedure

A known mass of anorthite (1.3 g) was introduced into the reactor on a Millipore filter of 0.22 μm pore-size, and reacted with a feed solution. The total ionic strength of the feed solution was adjusted to 0.05 $mol/dm^3$ by combining standard solutions of

$NaClO_4$ and $NaHCO_3$. Constant ionic strength was maintained in order to eliminate the effects of changing ionic strength on solution and surface speciation and on the liquid-junction potential of the electrode system used to monitor pH.

All salts used were of pro analysi or higher quality. Feed solutions were maintained in equilibrium with high quality gas mixtures (AGA Gas) with a composition known within 0.2%. The compressed gas was introduced into the feed solution vessels (1 l volume) by bubbling slowly from a 2 mm feed tube immersed in the solution. Feed solutions were maintained at the same temperature as the reactors. The $CO_2$ gas was washed by bubbling through 10% sulphuric acid followed by the ionic medium at the temperature used in the experiment in order to saturate the gas with water. The $N_2$ gas was washed in the same way but with an additional washing in 10% NaOH. Solution flowrate through the reactor was maintained near 2.5 ml/h. Samples of the outflow were taken regularly over a period of 6–7 weeks, the time needed to reach a constant outflow concentration for each ion. After acidification with $HNO_3$ the samples were stored until the end of the experiment, when all samples were analyzed at one time. Aluminum, Ca and Si concentrations were determined by Inductively Coupled Plasma Atomic Emission Spectroscopy (ICP-AES) on an ARL (Applied Research Laboratories) model 3520 B ICP analyzer. Analyses of samples were compared with calibration curves obtained from measurements on standard solutions containing $Al^{3+}$, $Ca^{2+}$ and $H_4SiO_4$ prepared with acidified solution media of the same ionic composition as used in the experiments. No correction for interelement interference was necessary.

The pH of the reactor outflow was measured on line after the reactor in a small flow-through measurement cell using a glass electrode–reference electrode pair of the type: (Ag(s),AgCl(s),$AgNO_3$/$NaClO_4$//test solution//glass electrode. The glass measurement cell contributed to a low background contamination of silicon as observed when feed solutions were run through the experimental setup in the absence of reacting mineral. All samples concentrations were subsequently corrected for this systematic error in Si concentration by subtracting the amount released in the absence of anorthite. On average the error contributed to 37% of the total Si signal. In all cases the corrected Si signal was at least 6 times the detection limit. This study focuses on the slower, rate-determining release of Al from the anorthite surface. We demonstrate below that there are no reaction products, such as secondary minerals, that affect Al release rates.

The kinetics of anorthite dissolution in the presence of $CO_2$ was studied first. Feed solutions were maintained at a fixed $PCO_2$ of 0.097 atm and 0.0097 atm (referred to as 0.1 and 0.01 atm in the text) respectively. The experiments were performed at various pH conditions ($5.5 < pH < 8.3$) depending on the $PCO_2$ selected, and the concentration of $HCO_3^-$ in the feed solution.

The second set of anorthite-experiments (a total of two at two different pH) was conducted in a glove box under $N_2$(g) atmosphere using the feed solution: $[Na^+] + [H^+] = [OH^-] + [ClO_4^-] = 0.05$ M. Feed solution pH was calculated from Gran titration (Gran, 1981) with residual acidity determinations to be pH $5.5 \pm 1$ and $8.5 \pm 1$. Due to slow glass electrode response and low buffer capacity at these proton concentrations there is an associated high uncertainty in measured pH. An additional experiment at the lower pH condition was carried out in order to confirm reproducibility of pH measurements and Al release.

The pH and bicarbonate and carbonate ion concentrations were calculated directly from the following $CO_2$(g)/$H_2O$ equilibria where $PCO_2$ and bicarbonate concentration were experimentally fixed:

$$CO_2(g) + H_2O = HCO_3^- + H^+ \quad pK_{a1} = 7.66\ (25°C, 0.05\ M\ NaClO_4) \tag{1}$$

$$CO_2(g) + H_2O = CO_3^{2-} + 2H^+ \quad pK_{a2} = 17.64\ (25°C, 0.05\ M\ NaClO_4) \tag{2}$$

Thermodynamic constants taken from Bruno et al. (1992) had been adjusted for ionic strength effects with the Specific Interaction Theory (Stumm and Morgan, 1981, p. 412; Grenthe et al., 1992).

### 2.4. Solid phase analysis

The anorthite surfaces were compared before and after experiments using scanning electron mi-

croscopy (SEM), SEM microprobe analysis and X-ray powder diffraction (XPD) (Philips PW 1130/00) with a detection limit of 5%. Solution compositions of the reactor effluents were entered into the geochemical code PHREEQE (Parkhurst et al., 1980). The code was used to calculate aqueous speciation using the original WATEQ thermodynamic data base (Trusdell and Jones, 1974) and the subsequent revisions that are critically reviewed by Nordstrom et al. (1991). Calculation results included the degree of saturation with respect to possible secondary mineral phases, and were reported as the ratio log $((IAP)/(K_{SO}))$ where $K_{SO}$ is the conditional solubility constant for a particular phase, and the IAP is the corresponding ion activity product.

## 3. Results

### *3.1. Anorthite dissolution rates in the presence and absence of $CO_2(g)$*

Fig. 1a shows the release rate for Al, Si and Ca vs. time for one of the carbon dioxide-experiments. An initial rapid release of all three elements is followed by a slowly decreasing release rate that seemingly approaches steady-state on the time-scale of these experiments. The dissolution is non-stoichiometric in all the experiments, with Al rates always slower than that predicted from stoichiometric release with respect to Si. For experiments with the fastest steady-state Al dissolution rates, Al and Si rates approach stoichiometric release. Fig. 1b shows the cumulative release of all elements with time. Aluminum release is much less than Si and Ca. The cumulative release of Al increases approximately linearly with time, while Si release is parabolic and plots as a straight line against $t^{1/2}$ (not shown) (for further discussion see Section 4).

Fig. 2a–c shows the effect of pH on the dissolution rate of anorthite in the presence and absence of $CO_2(g)$. Calcium- and Si-release rates show no pronounced dependence on pH in either case. Aluminum release is similar under $N_2(g)$ and $CO_2(g)$ at pH 5, and shows no pronounced dependence on pH under $N_2(g)$. These results are consistent with those of Amrhein and Suarez (1988) who found the rate of anorthite dissolution to be independent of pH in the range $5 < pH < 9$ under $N_2(g)$. The extensive compilation of aluminosilicate mineral dissolution rates of Sverdrup (1990) generally shows dissolution kinetics that are independent of pH in this range; i.e., our results under $N_2(g)$ are consistent with previous results for feldspar dissolution in the absence of carbon dioxide.

Aluminum release is dramatically higher in the presence of $CO_2(g)$ above pH 5, showing a strong

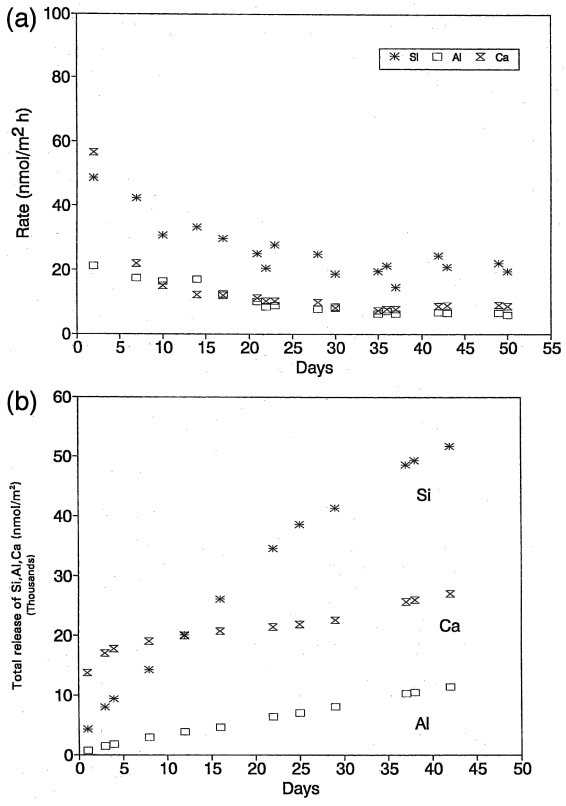


Fig. 1. (a) Release of Al, Si and Ca from anorthite as a function of time at $PCO_2 = 0.0097$ atm and pH = 8.1 in 25 mM $NaHCO_3$ + 25 mM NaClO. Values for dissolution rate correspond directly to reactor outflow concentration ($C$, mol/l). For the thin-film reactor, dissolution rate ($R$; mol/h) is obtained by multiplying outflow concentration by flow-rate ($F$, l/h); $R = CF$. Taking all experiments into consideration, the error in a single point, corresponding to propagation of analytical uncertainty, was at the most 1%, 1% and 5% for Si, Ca and Al respectively. Reported rates from all the experiments are taken as an average of the measured rates during quasi-steady-state. The uncertainty in calculated average rates was typically 10%. (b) Plot of cumulative release versus time. Cumulative Al release is nearly linear with time, while Si release is proportional to the square root of time.

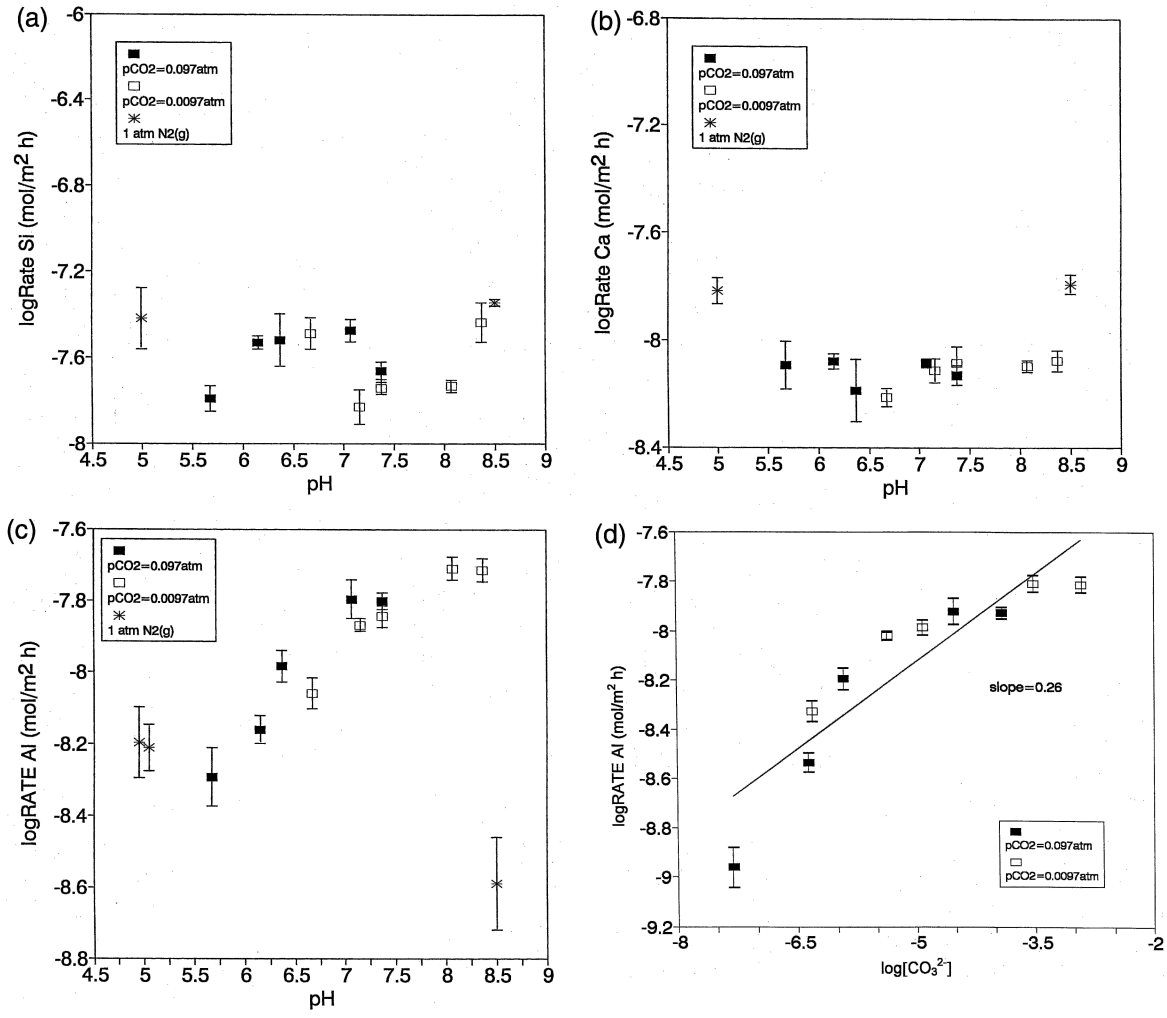


Fig. 2. Log dissolution rate of anorthite in terms of: (a) Si, (b) Ca and (c) Al, as a function of pH. (d) Log carbonate-accelerated dissolution rate of Al as a function of $\log[CO_3^{2-}]$. The error bars represent the 95% confidence interval.

effect from dissolved inorganic carbon. Experiments carried out at different $PCO_2$ can be compared for the results near pH 7. Although there is a clear trend of increasing Al release rate with pH in the presence of carbon dioxide, the effect of increasing $PCO_2$ from 0.01 atm to 0.1 atm at pH 7 is not dramatic. This is expected, and arises due to speciation effects where the master variable pH plays a much larger role than that of $PCO_2$ in determining the solubility of carbon dioxide, the distribution of reactive dissolved carbon species, and thus Al release rates (discussed below).

We tested for kinetic and transport control of reaction rate by, after approximately 46 days of pumping at an average flow rate of 2.5 ml/h, doubling the flow rate. After 4–5 days we took two more samples. Table 2 lists the release rates for Al, Si and Ca during steady-state with a flow rate of 2.5 ml/h vs. the release at doubled flow rate. Aluminum release rate is not affected by the increased flow rate; doubling the flow rate corresponded to decreasing the Al concentration in the reactor outflow by almost exactly one-half. As discussed by Dibble and Tiller (1981) and Chou and Wollast (1985a; b), *dissolution*

Table 2
Experimental flow-rates and corresponding dissolution-rates (during steady-state) of anorthite in the presence of 1% $CO_2$(g)

| pH | Flow [ml/h] | Day | $Rate_{Al}$ | $Rate_{Si}$ [nmol/m$^2$ h] | $Rate_{Ca}$ |
|---|---|---|---|---|---|
| 6.7 | 2.7 ± 0.1 | 29–46 | 8.8 ± 0.9 | 33.0 ± 7 | 6.2 ± 0.6 |
| | 5.1 | 50 | 8.5 | 53.2 | 5.7 |
| 7.4 | 2.5 ± 0.08 | 38–46 | 14.4 ± 0.7 | 17.6 ± 1 | 8.2 ± 1 |
| | 4.4 | 50 | 15.1 | 25.6 | 10.1 |
| | 3.7 | 51 | 13.3 | 25.1 | 17.6 |
| 8.1 | 2.5 ± 0.06 | 39–46 | 19.2 ± 1 | 19.0 ± 0.5 | 8.0 ± 0.3 |
| | 4.4 | 50 | 22.6 | 27.8 | 10.1 |
| | 3.7 | 51 | 18.2 | 19.5 | 8.3 |
| 8.4 | 2.5 ± 0.1 | 22–46 | 18.9 ± 1 | 38.2 ± 12 | 8.1 ± 0.6 |
| | 4.9 | 50 | 20.6 | 54.0 | 9.8 |
| | 4.8 | 51 | 20.8 | 60.8 | 8.8 |

*rates* that are independent of flow-rate must be independent of reaction product concentration, thus indicating that reaction products do not back-react with the mineral surface, and that the surface chemical reaction releasing reaction products to the mineral–solution interface is rate-limiting.

For transport-controlled dissolution, rates of Fickian diffusion are proportional to the concentration gradient between the mineral surface and the bulk of the solution, and thus depend on solution composition. Because the solution concentrations of reaction products decrease with increased flow rates, diffusion-controlled release will likewise increase with flow rate, although not proportionally. This behaviour is observed for Si in Table 2, other than the experiment at pH 8.1 where release rate changes little with flow rate, and for Ca except for the experiment at pH 6.7 where release rate changes little with flow rate (noting that the release rates of Ca at accelerated flow are in several cases nearly within the standard error reported for the dissolution rate under slower flow). To conclude, Al release is surface reaction controlled, while the rate controlling mechanism is less conclusive for Si and Ca but appears in most cases to be diffusion controlled, possibly exhibiting mixed kinetics where neither rate-controlling mechanism dominates the overall energetics of Si or Ca release to solution.

### 3.2. Stoichiometry of dissolution

Table 3 shows the accumulated release of Al, Si and Ca from the anorthite. In all cases total Al release is less than that of Si; i.e., the dissolution is non-stoichiometric for the network-forming cations Al and Si, with an apparent depletion of Si at the

Table 3
Cumulative release of Al, Si and Ca from anorthite reacted under 10% $CO_2$(g) during 37 days
Equivalents of anorthite are calculated using the total moles of each element released and the corresponding stoichiometric coefficient for the composition of anorthite according to the electron microprobe analysis (Table 1).

| pH | Al [μmol/m$^2$] | Ca | Si | Al [μeq/m$^2$] | Ca | Si | Ca/Si [μeq]/[μeq] | Al/Si |
|---|---|---|---|---|---|---|---|---|
| 5.7 | 6.3 | 26 | 27 | 3.2 | 22 | 13 | 1.6 | 0.24 |
| 6.2 | 11 | 15 | 34 | 5.5 | 12 | 17 | 0.73 | 0.32 |
| 6.4 | 11 | 26 | 49 | 5.4 | 22 | 25 | 0.88 | 0.22 |
| 7.1 | 21 | 12 | 43 | 11 | 9.7 | 21 | 0.46 | 0.51 |
| 7.4 | 18 | 11 | 30 | 9.2 | 9.5 | 15 | 0.63 | 0.61 |

reacting mineral–water interface. This result is broadly in agreement with previous studies of bytownite, labradorite (Welch and Ullman, 1993) and oligoclase (Mast and Drever, 1987) dissolution which showed Al release to be slightly slower than Si for $5 < pH < 9$. These studies also showed that the presence of organic ligands accelerated Al release such that nearly stoichiometric release was obtained in the same pH range. These results are consistent with our data plotted in Fig. 3, which show Al release to be accelerated sufficiently that release rates approach values that are stoichiometric with those of Si at the highest Al release rates.

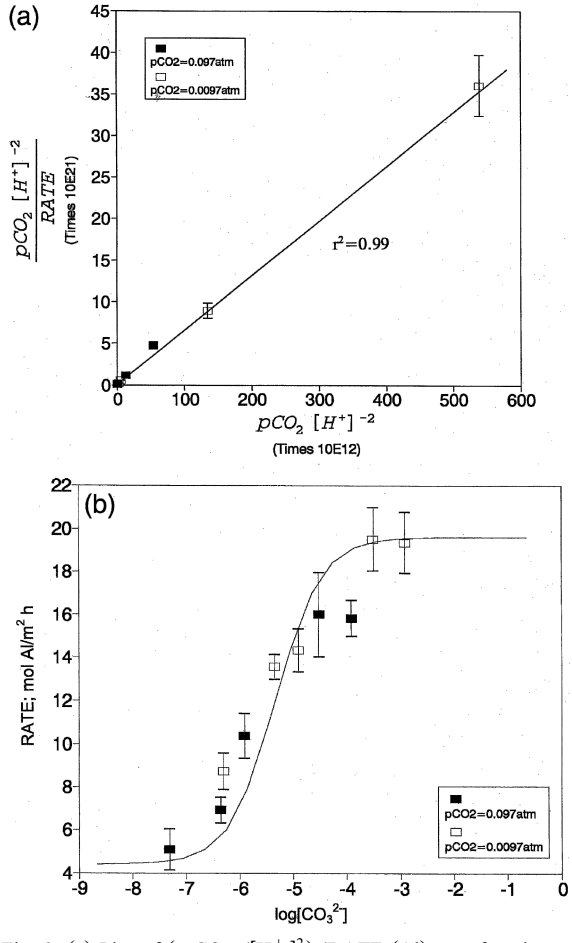


Fig. 3. (a) Plot of $(PCO_2/[H^+]^2)/\text{RATE (Al)}$ as a function of $(PCO_2/[H^+]^2)$. (b) Comparison of derived rate expression (solid line) with experimental data. The error bars represent the 95% confidence interval.

Aqueous speciation calculations show that the outflow solution in all the experiments was undersaturated with respect to amorphous $Al(OH)_3(s)$, calcite, halloysite ($Al_2Si_2O_5(OH)_4(s)$) and amorphous silica. The ion activity product, IAP, corresponding to the solubility of calcite and silica was smaller than the solubility constant, $K_{SO}$, by a factor of, on average, $10^{3.1}$ and $10^{2.5}$, respectively. The IAP corresponding to $Al(OH)_3(a)$ and halloysite was smaller than $K_{SO}$ by a factor of, on average, $10^{1.1}$ and $10^{1.7}$, respectively, but was in two extreme cases smaller than $K_{SO}$ by a factor of only 3.5. Outflow solutions were oversaturated with respect to kaolinite by a factor $10^2$ on average, but were approximately at saturation in two of the experiments. X-ray powder diffraction analyses of reacted anorthite samples showed no crystalline phases other than anorthite.

Scanning electron microscopy (SEM) and SEM backscatter imaging showed no neoformation of surface precipitates or enrichment of the reacted anorthite surface by reaction products. Some areas of the reacted surface showed limited spallation and possible formation of etch pits. These results and the flow-rate dependence presented above indicate that non-stoichiometric dissolution is unlikely to originate from precipitation or adsorption of reaction products. In this case, non-stoichiometric dissolution may result from multi-site dissolution reactions in parallel, where Si release is faster than Al, and therefore depleted relative to Al, at the mineral surface.

## 4. Discussion

The kinetic models of Schnoor (1990) and Malmström and Banwart (1997) predict that the rate of dissolution for the bulk anorthite framework will be accelerated if release of the slowest-dissolving framework ion is accelerated. The Schnoor model assumes that depletion of the more rapidly released framework ion, Si in our experiments, creates a depletion layer between the reacting surface and the solution, which grows until transport of Si across the layer becomes diffusion controlled. The depth of layer increases until the diffusion path is sufficiently long that Si release slows to the rate of Al release

which is controlled by surface chemical reaction kinetics. Acceleration of Al release by adsorbed ligands will thus lead to a more rapid stoichiometric dissolution. The model of Malmström and Banwart assumes that Si is also surface reaction controlled, and is proportional to the number of Si sites reacting at the surface. As Si becomes initially depleted, the release rate slows due to depletion of reactive sites. The number of sites continues to decrease until the Si release rate equals that of Al release. For both models, the slowest dissolving network ion is the best proxy for the long-term, stoichiometric dissolution of the mineral.

Acceleration of Al release by carbonate ligands therefore corresponds to accelerated (and eventually stoichiometric) dissolution of the anorthite. Earlier application of Schnoor's model to anorthite dissolution suggests a time period of 2–5 years to reach stoichiometric dissolution (Berg and Banwart, 1994). It is straightforward to calculate the time to reach stoichiometric dissolution by using the model of Schnoor (1990). Applying the expressions for accumulation of Si ($[\mathrm{Si}] = k_{\mathrm{Si}} t^{1/2}$) and Al ($[\mathrm{Al}] = k_{\mathrm{Al}} t$) in solution, and setting their first derivatives equal, yields an expression that can be explicitly solved for time: $\mathrm{d}[\mathrm{Si}]/\mathrm{d}t = \mathrm{d}[\mathrm{Al}]/\mathrm{d}t$, $1/2 k_{\mathrm{Si}} t^{-1/2} = k_{\mathrm{Al}}$. The values of $k_{\mathrm{Si}}$ and $k_{\mathrm{Al}}$ are determined as straight line slopes by linear regression of plots of [Si] vs. $t^{1/2}$ and [Al] vs. $t$, respectively. Malmström and Banwart (1997) predict a time period of several decades for the dissolution of biotite to become stoichiometric under the reported reaction conditions. Both models explain the non-stoichiometric dissolution observed in these experiments as reflecting the individual release rates for Al and Si during initial development of the reacting layer. This initial non-stoichiometric dissolution reaches a quasi steady-state during which further, much slower development of the Si-depleted reacting layer leads to stoichiometric dissolution over a period of years. This transition from the quasi steady-state to stoichiometric dissolution is too slow to be observed over the time scale of these experiments.

### 4.1. Rate dependence on aqueous carbon species

The trend of increasing Al release rate with increasing pH qualitatively correlates with the increasing concentration of total dissolved carbon, hydrogen carbonate ion and carbonate ion, with pH for an open $CO_2(g)$–$H_2O$ system (Stumm and Morgan, 1981, pp. 180–182). The stoichiometry between protons and dissolved carbon dioxide for the reacting species can be assessed by quantitatively comparing trends in carbonate-accelerated dissolution rate with hydrogen carbonate ion and carbonate ion, respectively. We calculated the rate of carbonate-accelerated dissolution of anorthite by subtracting the rate observed in the absence of $CO_2$ from the total rate ($R_{\mathrm{tot}}$). The dissolution rate of Al in the absence of $CO_2$ is estimated by the average rate from the two determinations at pH 5.5 and 8.5 (a total of three experiments); $R_0 = 4.4 \times 10^{-9}$ mol/m$^2$ h. Eq. (2) expresses the carbonate-promoted dissolution of anorthite in terms of $R_{\mathrm{tot}}$ and $R_0$ where $R_{\mathrm{c}}$ is the rate of carbonate-promoted dissolution of Al sites and $R_0$ is the rate of dissolution of Al sites unoccupied by carbonate ligands:

$$R_{\mathrm{C}} = R_{\mathrm{tot}} - R_0 \tag{3}$$

The increase in the rate of aluminum release correlates well with the dissolved carbonate ion concentration. Fig. 2d shows the logarithm of the rate of carbonate-accelerated dissolution plotted against the logarithm of carbonate ion concentration.

The correlation with carbonate concentration is represented by the empirical rate law $\mathrm{Rate}_{\mathrm{C}} = k[\mathrm{CO}_3^{2-}]^n$. Linear regression of the data plotted in Fig. 2d yields $k = (1.1 \pm 1) \cdot 10^{-7}$ and $n = 0.24 \pm 0.001$ (error limits quoted correspond to the 95% confidence interval). Combining the mass law for carbonate ion equilibrium (Eq. (2)) with this rate law, by eliminating the variable $[\mathrm{CO}_3^{2-}]$, yields the following Eq. (4) also written in logarithmic form (5) where the activity of water is assumed unity. This form of the rate law avoids calculating solution speciation and shows the direct dependence of dissolution rate in terms of the two master variables pH and $P\mathrm{CO}_2$:

$$\mathrm{Rate}_{\mathrm{C}} = k \left( \frac{P\mathrm{CO}_2 [\mathrm{H}_2\mathrm{O}] K_{\mathrm{a2}}}{[\mathrm{H}^+]^2} \right)^n \tag{4}$$

$$\log(\mathrm{Rate})_{\mathrm{C}} = \log k - 0.24\, \mathrm{p}K_{\mathrm{a2}} + 0.24 \log(P\mathrm{CO}_2) + 0.48\, \mathrm{pH} \tag{5}$$

This rate law predicts only a weak dependence of dissolution rate on $PCO_2$. At fixed pH, the effect of a 1 order-of-magnitude increase in $PCO_2$ would lead only to a 38% increase in dissolution rate. Increasing pH by 1 unit at fixed $PCO_2$ would increase the rate by 91%. At pH 7, values of $PCO_2$ would have to drop by 3 orders-of-magnitude (to $\sim 10^{-4}$ atm) in order to decrease Al release rates to those observed under $N_2$(g). Alternatively, increasing hydrogen ion concentration by 1–2 orders-of-magnitude to around pH 5 decreases the dissolution rate to that observed under $N_2$(g). This effect emphasizes that rates increase with carbonate ion concentration, which in turn is more sensitive to pH than $PCO_2$ for an open $CO_2$(g)–$H_2O$ system.

The fractional reaction order for $[CO_3^{2-}]$ ($n = 0.24$) is consistent with surface–chemical-reaction controlled dissolution, where the reaction rate is proportional to the surface concentration of reactive sorbates (Grauer and Stumm, 1982; Blum and Lasaga, 1988; Wieland et al., 1988). Fractional-order dissolution kinetics arises from the adsorption behavior of many solutes which can be described by the Freundlich isotherm, $C_s = K_f C_{(aq)}^{1/m}$, where $C_s$ is surface concentration (mol $m^{-2}$), $C_{(aq)}$ is solution concentration (mol $l^{-1}$) and $K_f$ and $m$ are empirical constants with $1/m$ generally less than 1 for monolayer adsorption (Adamson, 1990). Substituting the expression for surface concentration directly into a first-order rate law written in terms of surface concentration, $R = kC_s$, would result in a fractional-order rate dependence of the form $R = kK_f C_{(aq)}^{1/m}$, with $1/m < 1$.

Fractional-order kinetics corresponds to an adsorption saturation effect where surface concentration of the reactive species starts to level off at higher concentrations of solution species, due to the approach to monolayer coverage for the reactive adsorbate species. Because reaction rates are proportional to surface concentrations of reactive species, they likewise show a saturation effect; i.e., dissolution rates level off at higher concentrations of the dissolved species. Fractional-order kinetics or saturation effects for dissolution rates have been observed for a number of mineral dissolution studies that showed a corresponding *integral-order rate dependence on the surface concentration* of protons (Furrer and Stumm, 1986; Zinder et al., 1986; Amrhein and Suarez, 1988; Blum and Lasaga, 1988Blum and Lasaga, 1991; Carroll-Webb and Walther, 1988; Wieland et al., 1988; Wieland and Stumm, 1992; Oxburgh et al., 1994), ligands (Furrer and Stumm, 1986; Zinder et al., 1986; Amrhein and Suarez, 1988) or reductants (Banwart et al., 1989; Hering and Stumm, 1990).

### *4.2. Proposed mechanism and resulting rate expression*

The correlation between Al release rate and dissolved carbonate ion concentration, and the fractional-order rate dependence, are explained by considering adsorption of carbonate ion. Furrer and Stumm (1986) demonstrated that the dissolution rate of aluminum oxide was proportional to the surface concentration of adsorbed ligands that accelerated the release of Al from the surface. We tested this hypothesis for carbonate-accelerated dissolution of anorthite by deriving a rate expression where the rate of Al release is proportional to the surface concentration of carbonate ligand. Eq. (6) describes the adsorption of carbonate ion at hydrated Al sites on the anorthite surface:

$$> AlOH_2^+ + CO_3^{2-} \Rightarrow AlCO_3^- + H_2O \qquad (6)$$

Combining this reaction with Eq. (2) for the deprotonation of hydrated $CO_2$(g) to form carbonate ion allows us to write formation of the surface complex in terms of the experimentally-fixed master variables $PCO_2$ and pH. Eq. (7) is the thermodynamic mass law obtained from combining Eqs. (6) and (2). Eq. (8) is the corresponding stoichiometric reaction:

$$K_s = \frac{\{> AlCO_3^-\}[H^+]^2}{\{> AlOH_2^+\} PCO_2}; \qquad (7)$$

We therefore write the overall dissolution of Al in two steps: rapid establishment of pre-equilibrium for formation of the reactive Al–carbonate complex (Eq. (8)), followed by slow, irreversible detachment of the metal complex from the surface (Eq. (9)):

$$> AlOH_2^+ + CO_2 \Rightarrow AlCO_3^- + 2H^+ \quad K_s \qquad (8)$$

$$> AlCO_3^- \rightarrow \text{new surface site} + Al_{(aq)} \qquad (9)$$

Eq. (10) is the kinetic law of mass action for detachment of the Al–carbonate complex to solution:

$$\frac{d[\mathrm{Al}]_{\mathrm{tot}}}{A\,dt} = k\{ > \mathrm{AlCO_3^-}\} \ (\mathrm{mol/m^2}) \qquad (10)$$

$A$ ($\mathrm{m^2}$) is total surface area of reacting anorthite. $k$ ($\mathrm{h^{-1}}$) is the first order rate constant and $\{\mathrm{AlCO_3^-}\}$ ($\mathrm{mol/m^2}$) is the surface concentration of the Al–carbonate complex.

This mechanism has been demonstrated previously for the ligand-accelerated dissolution of aluminum oxide by combining wet chemistry techniques with fluorescence spectroscopy of reactive Al–ligand complexes (Hering and Stumm, 1990). The authors showed rapid formation of the reactive surface complex, much slower release of the surface Al–ligand complex to solution, and linear accumulation of Al in solution with time. They demonstrated that linear kinetics corresponds to (1) a constant concentration of the surface Al–ligand complex maintained in equilibrium with free ligand in solution, and (2) a constant steady-state concentration of active dissolution sites that were renewed as Al was released to solution.

For ligand-accelerated dissolution of anorthite, formation of the Al–carbonate complex can be modeled by combining the thermodynamic mass law (7) with a mass balance for surface Al species (Eq. (11)). This modeling approach has been previously applied to the ligand-accelerated dissolution of aluminum oxide (Pulfer et al., 1984), the proton-accelerated dissolution of albite (Blum and Lasaga, 1988) and calcic feldspars (Stillings and Brantley, 1995), and the reductive dissolution of iron oxide by Fe(II) complexes (Suter et al., 1991), ascorbate (Banwart et al., 1989) and hydrogen sulfide (Dos Santos and Stumm, 1992). In order to find a reaction mechanism consistent with our experimental data, we systematically tested possible combinations of reacting surface species (see Section 4.3). All models other than the one presented below failed to provide a correlation between reaction rate and the surface concentration of the reactive species.

Eq. (11) defines the mass balance for total reactive Al-sites ($S_t$) over the pH-range studied:

$$S_t = \{ > \mathrm{AlOH_2^+}\} + \{ > \mathrm{AlCO_3^-}\} \ (\mathrm{mol/m^2}) \qquad (11)$$

The following expression for formation of the surface Al–carbonate complex is obtained by combining Eqs. (7) and (11):

$$\{ > \mathrm{AlCO_3^-}\} = \frac{K_s S_t \left( P\mathrm{CO_2}/[\mathrm{H^+}]^2 \right)}{1 + K_s \left( P\mathrm{CO_2}/[\mathrm{H^+}]^2 \right)} \qquad (12)$$

Eq. (12) defines the adsorption isotherm for inorganic carbon, and is similar in mathematical form to the Langmuir isotherm. Implicit in the Langmuir isotherm is the assumption that all unoccupied surface sites have the same binding energy for the adsorbate species. In our model, this corresponds to unoccupied adsorption sites that are described by a unique free energy of formation and are thus represented by a single surface chemical species; $> \mathrm{AlOH_2^+}$.

Substituting Eq. (12) into Eq. (10) gives a rate expression for carbonate-promoted dissolution, $R_C$, defined in terms of the experimentally fixed master variables $[\mathrm{H^+}]$ and $P\mathrm{CO_2}$:

$$R_C = \frac{k\left( K_s S_t \left( P\mathrm{CO_2}/[\mathrm{H^+}]^2 \right) \right)}{1 + K_s \left( P\mathrm{CO_2}/[\mathrm{H^+}]^2 \right)} \qquad (13)$$

The surface chemical coordination theory for dissolution kinetics expresses the total dissolution rate as the sum of contributions from each reactive surface species dissolving in parallel reactions (Stumm and Furrer, 1987; Stumm and Wieland, 1990; Stumm and Wollast, 1990). The total rate of ligand-accelerated dissolution ($R_{\mathrm{tot}}$) is the sum of the release rates for surface sites complexed by the ligand ($R_L$) and that for unoccupied sites ($R_0$); $R_{\mathrm{tot}} = R_L + R_0$ (Pulfer et al., 1984; Furrer and Stumm, 1986; Zinder et al., 1986; Amrhein and Suarez, 1988; Wieland and Stumm, 1992). Our surface complexation model considers two surface species; unoccupied sites and surface Al–carbonate complexes. We calculated the rate of carbonate-accelerated dissolution of anorthite, $R_C$, by subtracting the rate observed in the absence of $\mathrm{CO_2}$ from the total rate ($R_{\mathrm{tot}}$) (see Eq. (3)). A rate expression for carbonate-accelerated dissolution alone can now be compared with the rate, $R_C$, obtained from the experimental data.

Taking the reciprocal of both sides of Eq. (13) and then multiplying each side with $(P\mathrm{CO_2}/[\mathrm{H^+}]^2)$

gives the following linear equation for $(PCO_2/[H^+]^2)/R_C$ as a function of $(PCO_2/[H^+]^2)$:

$$\frac{\left(PCO_2/[H^+]^2\right)}{R_C} = \frac{1}{kK_sS_t} + \frac{\left(PCO_2/[H^+]^2\right)}{kS_t} \quad (14)$$

A plot of the experimental data according to Eq. (14) should give a straight line with intercept $= 1/(K_s kS_t)$ and slope $= 1/(kS_t)$.

### 4.3. Determination of model parameters

Fig. 3a shows the experimental data plotted in the form $(PCO_2/[H^+]^2)/R_C$ vs. $(PCO_2/[H^+]^2)$. The data is linearized by the double-reciprocal plot. Linear regression of the data plotted in Fig. 4a provides a fit of all data to Eq. (15) and yields a value of $\log K_s = -12 \pm 1$ and $(kS_t) = (1.5 \pm 0.05) \times 10^{-8}$ (error limits quoted correspond to the 95% confidence interval). The corresponding value of Ks for formation of the Al–carbonate complex given by Eq. (6) is $\log K_s = 5.3 \pm 1$.

Fig. 3b shows the total rate of dissolution plotted as a function of $\log(CO_3^{2-})$. There is a slight disagreement between the data obtained at different $PCO_2$ at high carbonate concentration which may suggest two different rate maxima. In order to examine this possibility we systematically tested other models for the formation and reactivity of surface species, such as introducing competitive adsorption by $OH^-$. However, we found no plausible model which gave a fit better than the one we present here.

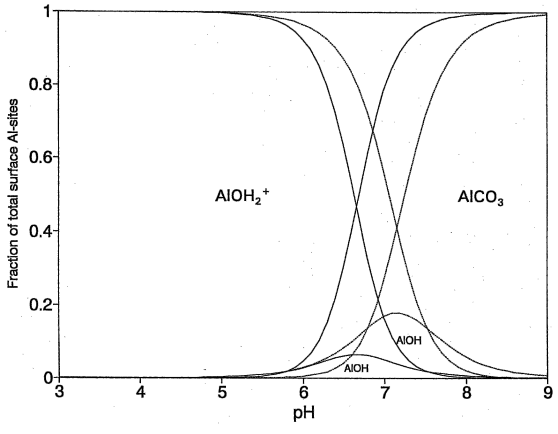


Fig. 4. Distribution diagram for surface speciation of Al-sites on anorthite. For a surface acidity constant of $p_sK_{a1} = 7.5$, deprotonated Al sites ( > AlOH) are minor species in the presence of $CO_2$ in the pH range studied. These sites can therefore be neglected in the mass balance for surface sites (Eq. (11)).

The stoichiometry of the surface Al–carbonate complex is well-constrained by the rate dependence on pH and $PCO_2$. We previously attempted to model hydrogen-carbonate adsorption with the reaction $> AlOH + HCO_3^- \Rightarrow AlCO_3^- + H_2O$ (or, combining this reaction with Eq. (3), $> AlOH + CO_2 \Rightarrow AlCO_3^- + H^+$) (Berg and Banwart, 1994). The data showed no consistent correlation between results obtained at 0.01 atm and 0.1 atm $CO_2$. We likewise rejected a model that considered formation of a protonated surface Al–carbonate complex: $> AlOH_2^+ + CO_2 \Rightarrow AlHCO_3 + H^+$. We tried all reasonable combinations of reactive species ($> AlOH_2^+$, $> AlOH$, $CO_2$(g), $HCO_3^-$, $CO_3^{2-}$) for formation of both protonated and deprotonated surface complexes ($> AlHCO_3$, $> AlCO_3^-$). The rate data *only* correlate with formation of a reactive complex having a 2:1 stoichiometry between protons and carbon, thus the proposed stoichiometry in Eq. (8).

This result is consistent with that of Furrer and Stumm (1986) who showed that the pH dependence of ligand-accelerated dissolution correlates with complete deprotonation of the adsorbed ligand, associated with forming a bi-dentate bond with surface Al sites. They postulate that such multi-dentate bonds are especially effective in polarizing and destabilizing the remaining bonds to the mineral lattice, thus lowering the activation energy for release to solution. Recently, Ludwig et al. (1995) elegantly demonstrated this chelate effect by showing a clear correlation between rates of ligand-accelerated dissolution for Nickel oxide, the rates of corresponding ligand-exchange reactions for metal complexes in solution and the effect of increasing chelation to accelerate both processes.

Carbonate adsorption on Al- and Fe-oxides has also been confirmed by IR and Raman spectroscopy; several studies have indicated that $CO_2$ adsorption on Al- and Fe-oxides occurs predominantly as $CO_3^{2-}$-ions. (Russell et al., 1975; White and Hem,

1975; Serna et al., 1977; Rochester and Topham, 1979; Zeltner and Anderson, 1988).

### 4.4. Surface speciation on complex minerals

Our conceptual approach to describing the anorthite surface is based on a number of previous studies where the kinetics of dissolution for complex silicate minerals is described by solute adsorption on the hydrous mineral surface (see review by Casey, 1990). The hydrous surface is generally assumed to be composed of a linear combination of sites, (e.g., hydroxo groups) Me–OH, whose corresponding acidity and complexation constants correlate with those for analogous binary oxides or solution complexes (Bales and Morgan, 1985; Carroll-Webb and Walther, 1988; Guy and Schott, 1989; Wieland and Stumm, 1992; Malmström and Banwart, 1997).

In our model of the anorthite surface, Al sites do not undergo deprotonation reactions in the pH range of our study. If we interpret the protonation state of Al sites on the anorthite surface as analogous to those for binary Al-oxides, we expect the first acidity constant to fall in the range $5.2 < p_s K_1 < 7.9$ (see Schindler and Stumm, 1987; data from Huang and Stumm, 1973 and Pulfer et al., 1984). Fig. 4 shows the distribution of surface Al-species as a function of pH, assuming a value of $p_s K_1 = 7.5$. Although deprotonated sites will dominate above pH 7.5 in the absence of adsorbed species other than protons and hydroxide ions, these would only be minor species in the presence of $CO_2$(g) since the Al–carbonate complex dominates the surface in this pH range. Based on these calculations along with those of Biber et al. (1994), which demonstrated the effect of ligand adsorption to shift the acidity of protonated surface sites giving *higher* conditional values for $p_s K_1$ as surface charge changes with ligand adsorption, we neglected deprotonated Al surface sites in the surface sites mass balance in Eq. (11).

### 4.5. A comparison of oxalate and carbonate ligand-promoted dissolution for plagioclase

Many investigators propose that it is organic ligands, such as those with carboxylic and phenolic functional groups, that cause accelerated weathering in soils (see review by Blum and Stillings, 1995). Our kinetic model for carbonate-accelerated weathering assumes that the rate of dissolution is proportional to the surface concentration of carbonate ligand. Although this effect may increase weathering rates in laboratory systems, it is not necessarily significant compared to the effect of organic ligands in natural systems. In order to test the significance of carbonate-promoted weathering, we have compared our results with published data on plagioclase weathering in solutions of oxalic acid. This compound is a

Table 4
A comparison of oxalate and carbonate ligand-promoted dissolution for plagioclase
The stoichiometric equations (* and **) provided the best fit to the experimental data. In the mass balance for surface sites, unoccupied sites were written as [> AlOH] and [> $AlOH_2^+$], respectively, corresponding to the proton stoichiometry in (*) and (**). Amrhein and Suarez (1988) reported their dissolution data in terms of release of Si. We assumed stoichiometric dissolution for Si and Al, and converted dissolution rate for Si ($R_{Si}$) to dissolution rate for Al by multiplying $R_{Si}$ with the ratio of the stoichiometric coefficients for Al and Si in the mineral (Al/Si mole ratio = 0.89).
The error limits given for the constants correspond to a 95% confidence interval.

| Mineral ligand | Ref. | $k$ [$10^{-3}$ $h^{-1}$] | $S_t$ | log $K_s$ | Observed rates [mole/$m^2$/h] |
|---|---|---|---|---|---|
| Anorthite oxalate | 1 | $3.1 \pm 0.3$ | a | $4.3 \pm 0.1$* | $-11.75 < \log R < -10.62$ |
| Bytownite oxalate | 2 | $10.5 \pm 1.0$ | a | $6.4 \pm 0.7$* | $-10.15 < \log R < -7.92$ |
| Anorthite carbonate | 3 | $0.25 \pm 0.1$ | a | $5.3 \pm 1.0$** | $-11.76 < \log R < -11.26$ |

1 — Amrhein and Suarez, 1988. Total ionic strength = 6.25 mmol/$dm^3$.
2 — Welch and Ullman, 1993. Total ionic strength = 2.5 mmol/$dm^3$.
3 — This study. Total ionic strength = 50 mmol/$dm^3$.
a — $S_t = (1.2 \times 10^{-4}$ mol/$m^2)^I \times (n\mathrm{Al}/(n\mathrm{Al} + n\mathrm{Si}))$; $n$ denotes stoichiometric coefficient. (I) from Amrhein and Suarez, 1988.
* — $K_s$ for: > $AlOH + HX^- \leftrightarrow AlX^- + H_2O$, $H_2X$ = oxalic acid.
** — $K_s$ for: > $AlOH_2^+ + X^{2-} \leftrightarrow AlX^- + H_2O$, $H_2X$ = carbonic acid.

low molecular weight di-carboxylic acid that is an analogue to many types of soil organic acids having carboxylic functional groups that can interact with mineral surfaces. It is well established in the studies described below that the oxalate ligand acts to accelerate plagioclase dissolution, particularly the release of Al.

We applied the rate expression derived above to published dissolution kinetic data for anorthite and bytownite. Literature data for ligand-promoted dissolution in the systems anorthite-oxalate (Amrhein and Suarez, 1988) and bytownite-oxalate (Welch and Ullman, 1993) were used to estimate the stability constant $K_s$, for the reactive complex, and the value of $(kS_t)$. Published values of $S_t$, determined independently, allow the first-order rate constant to be estimated.

Table 4 shows the result of the calculations. The rate constants for oxalate-promoted dissolution of the two plagioclase minerals are within a factor of 3. For anorthite, the rate constant for oxalate-promoted dissolution is approximately one order-of-magnitude larger than that for carbonate.

### *4.5.1. The effect of pH on carbonate and oxalate ligand-accelerated dissolution*

We calculated the rate of anorthite dissolution in the presence of either carbonate (this study), oxalate or protons (Amrhein and Suarez, 1988) as a function of pH. A soil $PCO_2$ of 1% and a total oxalate concentration of 100 μM reflects the upper range of field conditions in deeper soil layers and in surface organic soil layers, respectively (Appelo and Postma, 1993; Drever, 1994). The results, plotted in Fig. 5a, show that oxalate and protons are equally important in accelerating the dissolution at pH 4. For more acidic conditions, proton-promoted dissolution is by far the most dominant process. Oxalate-promoted dissolution dominates the overall dissolution rate between pH 4 and 6, while the effect of protons decreases dramatically and the effect of carbonate is negligible. Where the oxalate-promoted dissolution approaches zero between pH 6 and 7, the concentration of carbonate has reached values high enough to start accelerating the dissolution. At a pH of 9, carbonate-promoted dissolution has reached its maximum and the dissolution rate is five times that at pH 6. Fig. 5b compares the degree to which oxalate and

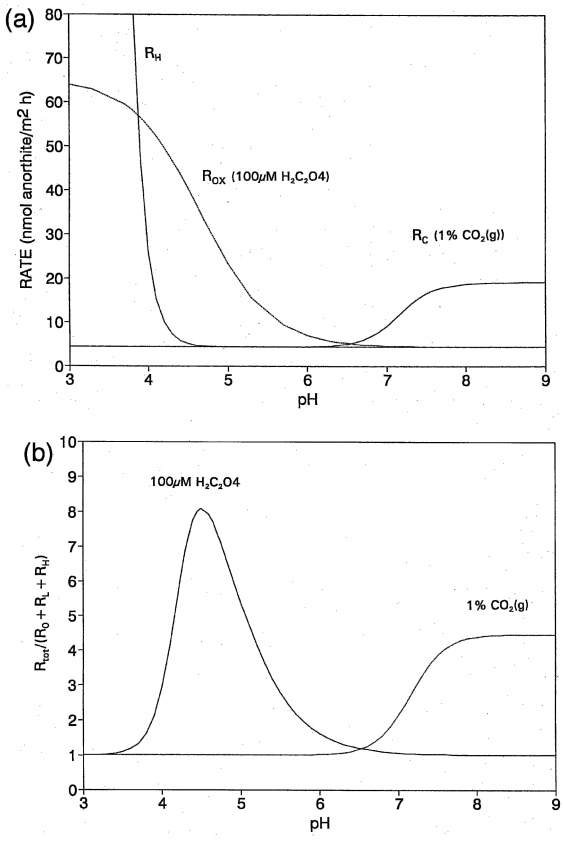


Fig. 5. (a) Dissolution-rate for anorthite as a function of pH at $T = 25°C$ in the presence of $CO_2$(g) ($R_C$), oxalate ($R_{Ox}$), or in the absence of reactive ligands other than protons ($R_H$): proton-accelerated dissolution (rate law from Amrhein and Suarez, 1988), $R_{tot} = k_H[H^+]^{2.7} + R_0$ (mol/m$^2$ h); $R_0 = 9\times10^{-9}$ mol Si/m$^2$ h and $k_H = 5.2\times10^3$ h$^{-1}$; oxalate-promoted dissolution (rate-law calculated from Si dissolution rate data from Amrhein and Suarez (1988) converted to Al dissolution rate by assuming stoichiometric dissolution), $R_{tot} = R_{ox} + R_0$ (mol Al/m$^2$ h); $R_0 = 8\times10^{-9}$ mol Al/m$^2$ × h and $R_{ox} = (kK_sS_t[C_2O_4H^-])/(1 + K_s[C_2O_4H^-])$ (see Table 4 for values of $k$, $K_s$ and $S_t$); carbonate-promoted dissolution as determined in this study; $R_{tot} = R_C + R_0$ (mol Al/m$^2$ ×h). See Eq. (13) for definition of $R_C$. $R_{tot}$ was normalized to the study by Amrhein and Suarez by multiplying $(kS_t)$ with the ratio $({}^1R_0/{}^2R_0)$, and exchanging ${}^2R_0$ for ${}^1R_0$. ${}^1R_0$ and ${}^2R_0$ represents $R_0$ in the study of Amrhein and Suarez and in this study, respectively. See Table 4 for values of $k$, $K_s$ and $S_t$. All three ''total rates'' were converted to dissolution of mol mineral/m$^2$ h by division with the stoichiometric coefficient for Si (2.09) or Al (1.86) in the anorthite mineral used by Amrhein and Suarez. (b) The ratio of $(R_{tot} = R_0 + R_{ligand} + R_H)$ to $(R_0 + R_H)$ as a function of pH for 100 μM oxalate (solid line) and 1% $CO_2$(g) (dashed line).

carbonate increase the dissolution relative to the rate in the absence of ligands, as a function of pH.

Although the results in Table 4 suggest that the reactivity of oxalate and carbonate is similar, these ligands affect the dissolution of anorthite in different pH-ranges. The large variation in dissolution rate with pH shown in Fig. 5a results from changes in aqueous speciation, that is concentration of respective reactive ligand ($[HC_2O_4^-]$ and $[CO_3^{2-}]$), with pH. There is a major difference between the speciation of organic ligands in general and that of carbonic acid in natural aquatic systems. The former are non-volatile acids while the latter can interact with a reservoir of $CO_2(g)$. Both the solubility of inorganic carbon and the carbonate ion concentration *increase* with pH for an open $CO_2(g)$–$H_2O$ system. For oxalate however, the concentration of the adsorbed ligand *decreases* with increasing pH into the near-basic and basic region (Balistrieri and Murray, 1987).

### 4.6. Implications for weathering in natural systems

We conclude that under laboratory conditions, carbonate can accelerate feldspar dissolution. If these weathering reactions qualitatively reflect field scale processes, we expect carbonate-promoted weathering to be most significant in environments with elevated $PCO_2$ and neutral to near-basic pH. Groundwaters, unsaturated zones in deep tills, and deep-ocean interstitial basalt waters are examples of such weathering environments. The possibility of carbonate-promoted feldspar dissolution should hence be considered in chemical weathering models for these type of waters.

Organic acids are assumed to contribute to the feedback between Ca- and Mg-silicate weathering and climate (Berner, 1992; Brady and Carroll, 1994; Drever, 1994). We have shown that under laboratory conditions carbonate can accelerate the dissolution of Ca-feldspar as effectively as organic acids. The effect of carbonate on Ca-feldspar weathering may hence have important implications for the weathering feedback in the geochemical carbon cycle. Based on this laboratory study we may, however, only conclude that carbonate ions has the *potential* to enhance anorthite weathering by a factor of 5. Although this may seem to be a weak effect, a corresponding enhancement of anorthite weathering due to increasing temperature requires a rise of 25°C (Brady and Carroll, 1994).

Carbonate-promoted dissolution may also be a possible explanation for two recently proposed weathering theories in the literature. First, Keller and Wood (1993) propose that subsurface microbial activity prior the advent of vascular plants on earth could have generated elevated partial pressures of $CO_2$ in the unsaturated zone that are comparable to values observed today. They conclude this may explain the historical weathering record, which indicates no significant change in weathering rates before and after the advent of vascular plants (Holland, 1984). If the field studies of Keller et al. (1991) reflect typical conditions in the deeper sub-surface, i.e., elevated $PCO_2$ values accompanied by neutral to near-basic pH conditions, $PCO_2$ has no direct effect on weathering in terms of proton-promoted dissolution. An alternative explanation for accelerated weathering in modern *or* pre-Silurian subsurface waters could be carbonate-promoted dissolution.

Secondly, Francois and Walker (1992) suggest submarine basalt weathering rather than continental silicate weathering as the major weathering feedback control on atmospheric $CO_2$ over geologic timescales. They assume that basalt weathering is proportional to deep-ocean total inorganic carbon concentration and $H^+$ concentration, which increases with increasing atmospheric $CO_2$ content. Since laboratory studies show no dependence between silicate weathering rates and pH in the neutral to near-basic pH region — the pH range of ocean water — the proposed effect of protons on basalt weathering has been questioned (Caldeira, 1995). Also the effect of inorganic carbon has been rejected in later studies (Berner, 1995; Caldeira, 1995) by reference to, on the one hand a kinetic study on olivine showing an inhibiting effect of $CO_2$ on dissolution rate at basic pH, and, on the other hand the study by Brady and Carroll (1994) showing no effect of $CO_2$ on weathering rate at acid pH. We show however that, at neutral pH, inorganic carbon can accelerate anorthite dissolution. Because plagioclase is a significant component of deep ocean basalt, results from anorthite weathering studies are relevant to these systems. Based on our laboratory results, the weathering of anorthite in deep-ocean basalt would be enhanced

almost five times compared to dissolution in the absence of carbonate ions, considering a ocean carbonate ion concentration of around 0.2 mM.

## 5. Conclusions

Anorthite weathering is accelerated in the presence of carbon dioxide. The dependence of dissolution-rate on pH and $PCO_2$ is consistent with the formation of a reactive surface Al–carbonate complex. We propose that the generally termed ''carbonation weathering'' should be extended to include not only proton-promoted weathering but also carbonate-promoted dissolution.

The contribution of carbonate, organic ligands and protons to mineral weathering in natural systems depends on the relative concentration of the reacting species and the reactivity of the various species formed; speciation must be considered. We conclude that in laboratory studies, carbonate ligand has the potential to accelerate dissolution rates to a degree comparable with organic ligands such as oxalate. We propose that the role of carbonate ligand should be considered in chemical models for feldspar weathering, and therefore in the proton balance and carbon cycle of natural waters. Carbonate may also have an important role in the geochemical carbon cycle through its contribution to the feedback between continental deep-ocean basalt weathering (continental and or deep-ocean basalt) and atmospheric $PCO_2$.

## Acknowledgements

A. Berg is supported by the Swedish Natural Science Research Council, # G-GU 6498-30X. S. Banwart was supported by the Swedish Nuclear Fuel and Waste Management for the duration of this project. *[SB]*

## References

Adamson, A.W., 1990. The Physical Chemistry of Surfaces. 5th edn., Wiley, New York, pp. 422–426.

Amrhein, C., Suarez, L., 1988. The use of a surface complexation model to describe the kinetics of ligand-promoted dissolution of anorthite. Geochim. Cosmochim. Acta 52, 2785–2793.

Appelo, C.A.J., Postma, D., 1993. Geochemistry, Groundwater and Pollution. A.A. Balkema, Rotterdam.

Bales, R.C., Morgan, J.J., 1985. Dissolution kinetics of chrysotile at pH 7 to 10. Geochim. Cosmochim. Acta 49, 2281–2288.

Balistrieri, L.S., Murray, J.W., 1987. The influence of the major ions of seawater on the adsorption of simple organic acids by goethite. Geochim. Cosmochim. Acta 51, 1151–1160.

Banwart, S., Davies, S., Stumm, W., 1989. The role of oxalate in accelerating the reductive dissolution of hematite ($\alpha$-$Fe_2O_3$) by ascorbate. Colloids Surf. 39, 303–309.

Berg, A., Banwart, A.S., 1994. Anorthite surface speciation and weathering reactivity in bicarbonate solutions at 25°C. Proceedings of the workshop ''$CO_2$ Chemistry'', Hemavan, Sweden, Sept. 13–16, 1993. Proceedings of the English Royal Society of Chemistry.

Berner, R.A., 1991. A model for atmospheric $CO_2$ over Phanerozoic time. Am. J. Sci. 291, 339–376.

Berner, R.A., 1992. Weathering, plants and the long-term carbon cycle. Geochim. Cosmochim. Acta 56, 3225–3231.

Berner, R.A., 1994. GEOCARB II: a revised model for atmospheric $CO_2$ over Phanerozoic time. Am. J. Sci. 294, 56–91.

Berner, R.A., 1995. Chemical weathering and its effect on atmospheric $CO_2$ and climate. In: White, A.F., Brantley, S.L. (Eds.), Chemical weathering rates of silicate minerals. Reviews in Mineralogy. Vol. 31, Mineralogical Society of America, Washington, DC, pp. 565–581.

Berner, R.A., Lasaga, A.C., Garrels, R.M., 1983. The carbonate-silicate geochemical cycle and its effect on atmospheric carbon dioxide over the past 100 million years. Am. J. Sci. 283, 641–683.

Biber, M.V., dos Santos Afonso, M., Stumm, W., 1994. The coordination chemistry of weathering: IV. Inhibition of the dissolution of oxide minerals. Geochim. Cosmochim. Acta 58, 1999–2010.

Blum, A.E., Lasaga, A.C., 1988. Role of surface speciation in the dissolution of minerals. Nature 331, 341–343.

Brady, P.V., 1991. The effect of silicate weathering on global temperature and atmospheric $CO_2$. J. Geophys. Res. 96 (B11), 18101–18106.

Brady, P.V., Carroll, S.A., 1994. Direct effects of $CO_2$ and temperature on silicate weathering. Possible implications for climate control. Geochim. Cosmochim. Acta 58, 1853–1856.

Brantley, S.L., Chen, Y., 1995. Chemical weathering rates of pyroxenes and amphiboles. In: White, A.F., Brantley, S.L. (Eds.), Chemical Weathering rates of silicate minerals. Reviews in Mineralogy. Vol. 31, Mineralogical Society of America, Washington, DC, pp. 565–581.

Bruno, J., Casas, I., Puigdomenech, I., 1991. The kinetics of dissolution of $UO_2$ under reducing conditions and the influence of an oxidized surface layer ($UO_{2+x}$): Application of a continuos flow-through reactor. Geochim. Cosmochim. Acta 55, 647–658.

Bruno, J., Stumm, W., Wersin, P., Brandberg, F., 1992. On the influence of carbonate in mineral dissolution: I. The thermodynamics and kinetics of hematite dissolution in bicarbonate solutions at T = 25°C. Geochim. Cosmochim. Acta 56, 1139–1147.

Caldeira, K., 1995. Long-term control of atmospheric carbon dioxide: low-temperature seafloor alteration or terrestrial silicate-rock weathering. Am. J. Sci. 295, 1077–1114.

Carroll-Webb, S., Walther, V., 1988. A surface complex reaction model for the pH-dependence of corundum and kaolinite dissolution rates. Geochim. Cosmochim. Acta 52, 2623–2699.

Casey, W.H., 1990. In: Hochella, M.F., White, A.F. (Eds.), Mineral–Water Interface Geochemistry. Reviews in Mineralogy. Vol. 23, Mineralogical Society of America, Washington, DC, 427.

Chou, L., Wollast, R., 1984. Study of the weathering of albite at room temperature and pressure with a fluidized bed reactor. Geochim. Cosmochim. Acta 48, 2205–2217.

Chou, L., Wollast, R., 1985a. Steady-state kinetics and dissolution mechanisms of albite. Am. J. Sci. 285, 963–993.

Chou, L., Wollast, R., 1985b. Study of the weathering of albite at room temperature and pressure with a fluidized bed reactor. Geochim. Cosmochim. Acta 49, 1659–1660.

Deng, Y., Banwart, S., 1994. Accumulation and remobilization of aqueous chromium(VI) at iron oxide surfaces. J. Cont. Hydrol.

Dibble, W.E., Tiller, W.A., 1981. Non-equilibrium water/rock interactions: I. Model for interface-controlled reactions. Geochim. Cosmochim Acta 45, 79–92.

Dos Santos Afonso, M., Stumm, W., 1992. Reductive dissolution of iron(III) (hydr)oxides by hydrogen-sulfide. Langmuir 8 (6), 1671–1675.

Drever, J.I., 1994. The effect of land plants on weathering rates of silicate minerals. Geochim. Cosmochim. Acta 58 (10), 2325–2332.

Francois, L.M., Walker, J.C.G., 1992. Modeling the phanerozoic carbon cycle and climate: constraints from the $^{87}Sr/^{86}Sr$ isotopic ratio of seawater. Am. J. Sci. 292, 81–135.

Furrer, G., Stumm, W., 1986. The coordination chemistry of weathering: I. Dissolution kinetics of $\delta$-$Al_2O_3$ and BeO. Geochim. Cosmochim Acta 50, 1847–1860.

Gran, G., 1981. Calculation of equivalence volumes in potentiometric titrations. Ph.D. Thesis. The Royal Inst. of Technology, Stockholm.

Grauer, R., Stumm, W., 1982. Die Koordinationschemie oxidischer Grenzflächen und ihre Auswirkung auf die Auflösungskinetic oxidischer Festphasen in wässerig Lösungen. Colloid Polym. Sci. 260, 959–970.

Grenthe, I., Fuger, J., Konings, R.J.M., Lemire, R.J., Muller, A.B., Nguyen-Trung, C., Wanner, H., 1992. Ionic strength corrections. Appendix B. In: Wanner, H., Forest, I. (Eds.), Chemical Thermodynamics of Uranium. North-Holland Elsevier, Amsterdam.

Guy, C., Schott, J., 1989. Multi surface reaction versus transport control during the hydrolysis of a complex oxide. Chemical Geology 78, 181–204.

Helgeson, H.C., Murphy, W.M., Aagaard, P., 1984. Thermodynamic and kinetic constraints on reaction rates among minerals and aqueous solutions: II. Rate constants, effective surface area and the hydrolysis of feldspar. Geochim. Cosmochim. Acta 48, 2405–2432.

Hering, J.G., Stumm, W., 1990. Oxidative and reductive dissolution of minerals. In: Hochella, M.F., White, A.F. (Eds.), Reviews in Mineralogy. Mineral–Water Interface Geochemistry. Vol. 23, Mineralogical Society of America, Washington, DC.

Holdren, G.R., Spyer, P.M., 1985. pH dependent change in the rates and stoichiometry of dissolution of an alkali feldspar at room temperature. Am. J. Sci. 285, 994–1026.

Holland, H.D., 1984. The Chemical Evolution of the Atmosphere and the Oceans. Princeton University Press.

Holland, H.D., Lazar, B., McCaffrey, M., 1986. Evolution of the atmosphere and the oceans. Nature 320, 27–33.

Huang, C.P., Stumm, W., 1973. Specific adsorption of cations on hydrous $\gamma$-$Al_2O_3$. J. Colloid Interface Sci. 43 (2), 409–420.

Keller, C.K., Wood, B.D., 1993. Possibility of chemical weathering before the advent of vascular plants. Nature 364, 223–225.

Keller, C.K., van der Kamp, G., Cherry, J.A., 1991. Hydrogeochemistry of a clayey till: 1. Spatial variability. Water Resour. Res. 27, 2543–2554.

Knauss, K.G., Wolery, T.J., 1986. Dependence of albite dissolution kinetics on pH and time at 25°C and 70°C. Geochim. Cosmochim. Acta 50, 2481–2497.

Lagache, M., 1965. Contribution a l'etude de l'alterationdes feldspaths, dans l'eau, entre 100 et 200°C, sous diverses pressions de $CO_2$, et application a la synthese des mineraux argileux. Bull. Soc. Fr. Mineral. Cristallogr. 88, 223–253.

Ludwig, C., Casey, W.H., Rock, P.A., 1995. Prediction of ligand-promoted dissolution rates from the reactivities of aqueous complexes. Nature 375, 44–46.

Malmström, M., Banwart, S.A., 1997. Biotite dissolution at 25°C: I. The pH-dependence of Dissolution Rate and Congruency. Geochim. Cosmochim. Acta.

Marshall, H.G., Walker, J.C.G., Kuhn, W.R., 1988. Long-term climate change and the geochemical cycle of carbon. J. Geophys. Res. 93, 791–801.

Mast, M.A., Drever, J.I., 1987. The effect of oxalate on the dissolution rates of oligoclase and tremolite. Geochim. Cosmochim. Acta 51, 259–2568.

Nordstrom, D.K., Plummer, L.N., Langmuir, D., Busenberg, E., May, H.M., Jones, B.F., Parkhurst, D.L., 1991. Revised chemical equilibrium data for major water-mineral reactions and their limitations. In: Melchoir and Bassett, R.L. (Eds.), Chemical Modeling of Aqueous Systems II, Chap. 31. American Chemical Society, Washington, DC, 398–413, ACS Symposium Series 416,

Oxburgh, R., Drever, J.I., Sun, Y.-T., 1994. Mechanism of plagioclase dissolution in acid solution at 25°C. Geochim. Cosmochim. Acta 58 (2), 661–669.

Parkhurst, D.L., Thorstenson, D.C., Plummer, L.N., 1980, PHREEQE-A computerized program for geochemical calculations. Water Resources Invest. 80–96, U.S. Geol. Survey.

Pulfer, K., Schindler, P.W., Westall, J.C., Grauer, R., 1984. Kinetics and mechanism of dissolution of bayerite ($\gamma$-$Al(OH)_3$) in $HNO_3$-HF solutions at 298.2 K. J. Colloid Interface Sci. 101 (2), 554–564.

Rimstidt, J.D., Dove, P.M., 1986. Mineral/solution reaction rates in a mixed flow reactor: wollastonite hydrolysis. Geochim. Cosmochim. Acta 50, 2509–2516.

Rochester, C.H., Topham, S.A., 1979. Infrared studies of the

adsorption of probe molecules onto the surface of goethite. J. Chem. Soc., Faraday Trans. 1 75, 872–882.

Russell, J.D., Paterson, E., Fraser, A.R., Farmer, V.C., 1975. Adsorption of carbon dioxide on goethite (α-FEOOH) surfaces, and its implications for anion adsorption. J. Chem. Soc., Faraday Trans. 1 71, 1623–1630.

Schindler, P.W., Stumm, W., 1987, The surface chemistry of oxides, hydroxides and oxide minerals. In: Stumm, W. (Ed.), Aquatic Surface Chemistry. Wiley-Interscience, New York, pp. 311–338.

Schlesinger, W.H., 1991. Biogeochemistry. An Analysis of Global Change. Academic Press, San Diego.

Schnoor, J.L., 1990. Kinetics of chemical weathering: A comparison of laboratory and field weathering rates. In: Stumm, W. (Ed.), Aquatic Chemical Kinetics. Wiley, New York.

Schnoor, J., Stumm, W., 1985. Acidification of aquatic and terrestrial systems. In: Stumm, W. (Ed.), Chemical Processes in Lakes. Wiley, New York.

Serna, C.J., White, J.L., Hem, S.L., 1977. Anion-aluminum hydroxide gel interactions. Soil Sci. Soc. Am. J. 41, 1009–1013.

Stillings, L.L., Brantley, S.L., 1995. Feldspar dissolution at 25°C and pH 3: reaction stoichiometry and the effect of cations. Geochim. Cosmochim. Acta 9, 1483–1496.

Stumm, W., Furrer, G., 1987. The dissolution of oxides and aluminum silicates; examples of surface-coordination-controlled kinetics. In: Stumm, W. (Ed.), Aquatic Surface Chemistry. Wiley-Interscience, New York.

Stumm, W., Morgan, J.J., 1981. Aquatic Chemistry. Wiley, New York.

Stumm, W., Wieland, E., 1990. Dissolution of oxide and silicate minerals; rates depend on surface speciation. In: Stumm, W. (Ed.), Aquatic Chemical Kinetics. Wiley-Interscience, New York.

Stumm, W., Wollast, R., 1990. Coordination chemistry of weathering. Rev. Geophys. 28, 53–69.

Suter, D., Banwart, S.A., Stumm, W., 1991. Dissolution of hydrous iron(III) oxides by reductive mechanisms. Langmuir 7 (4), 809–813.

Sverdrup, H., 1990. The Kinetics of Base Cation Release due to Chemical Weathering. Lund University Press.

Sverdrup, H., Warfvinge, P., 1993. Calculating field weathering rates using a mechanistic geochemical model — PROFILE. J. Appl. Geochem. 8, 273–283.

Trusdell, A.H., Jones, B.F., 1974. WATEQ — a computer program for calculating chemical equilibria of natural waters. J. Res. U.S. Geol. Surv. 2, 223–248.

Volk, T., 1987. Feedback between weathering and atmospheric $CO_2$ over the last 100 million years. Am. J. Sci. 287, 763–779.

Walker, J.C.G., Hays, P.B., Kasting, J.F., 1981. A negative feedback mechanism for the long-term stabilization of Earth's temperature. J. Geophys. Res. 86, 9776–9782.

Warfvinge, P., Sverdrup, H., 1992. Calculating critical loads of acid deposition with PROFILE — a steady-state soil chemistry model. Water, Air, Soil Pollut. 63, 119–143.

Welch, S.A., Ullman, W.J., 1993. The effect of organic acids on plagioclase dissolution rates and stoichiometry. Geochim. Cosmochim. Acta 57, 2725–2736.

White, A.F., Brantley, S.L., 1995. Chemical Weathering rates of silicate minerals. Reviews in Mineralogy, Vol. 31. Mineralogical Society of America, Washington, DC.

White, J.L., Hem, S.L., 1975. Role of carbonate in aluminum hydroxide gel established by Raman and IR analyses. J. Pharm. Sci. 64, 468–469.

Wieland, E., Stumm, W., 1992. Dissolution kinetics of kaolinite in acidic aqueous solutions at 25°C. Geochim. Cosmochim. Acta 56, 3339–3355.

Wieland, E., Wehrli, B., Stumm, W., 1988. The coordination chemistry of weathering: III. A generalization on the dissolution rates of minerals. Geochim. Cosmochim. Acta 52, 1969–1981.

Wogelius, R.A., Walther, J.V., 1991. Olivine dissolution at 25°C: Effects of pH, $CO_2$, and organic acids. Geochim. Cosmochim. Acta 55, 943–954.

Xie, Z., 1994. Surface properties of Silicates, their solubility and dissolution kinetics. Ph.D. Dissertation, Northwestern University, Evanston, IL.

Zeltner, W.A., Anderson, M.A., 1988. Surface charge development at the goethite/aqueous solution interface: effects of $CO_2$ adsorption. Langmuir 4, 469–474.

Zinder, B., Furrer, G., Stumm, W., 1986. The coordination chemistry of weathering: II. Dissolution of Fe(III)oxides. Geochim. Cosmochim. Acta 50, 1861–1869.